

## A COUPLED FINITE VOLUME SOLVER FOR THE SIMULATION OF DISPERSE MULTIPHASE FLOWS

**Marwan Darwish<sup>\*</sup>, Amer Abdel Aziz<sup>†</sup>, and Fadl Moukalled<sup>††</sup>**

<sup>\*</sup>American University of Beirut, Faculty of Engineering and Architecture  
Riad El Solh Street, Beirut, 1107 2020, Lebanon  
darwish@aub.edu.lb

<sup>†</sup>American University of Beirut, Faculty of Engineering and Architecture  
aka18@aub.edu.lb

<sup>††</sup>American University of Beirut, Faculty of Engineering and Architecture  
memouk@aub.edu.lb

**Key words:** Fluid Dynamics, Multiphase, Disperse, Coupled, FVM, Pressure-Based

**Abstract.** *In this paper a coupled multiphase finite volume collocated variable arrangements pressure based solver developed within a Eulerian-Eulerian framework is presented. The coupled solver differs from pressure based segregated solvers in that it accounts implicitly for the Pressure-Velocity and the inter-phase drag couplings that are present in disperse multiphase flows, thus yielding a system of coupled equations with velocity fields and pressure. Four test problems for dense and dilute disperse flows are shown to yield substantial decrease in the number of iterations to convergence as compared to a pressure based segregated multiphase solver.*

## 1 INTRODUCTION

Solution of fluid flow problems by pressure-based algorithms has been at the heart of interest of CFD research since Semi-Implicit Method for Pressure Linked Equations (SIMPLE) was developed by the CFD group at the Imperial college [1]. SIMPLE has been preferred by CFD researchers due to its simplicity of implementation and low memory requirements, a fact that encouraged the development of a group of SIMPLE-like algorithms which were proven to share similar behaviors by the authors [2]. Being segregated in nature, these algorithms are very dependent on the grid density and the under-relaxation value used. In general, the denser the mesh, the more iterations are needed to reach convergence. Besides, a high under-relaxation value is usually needed to promote convergence.

With the huge advancement in computer power in the last two decades, there has been a renewed interest in the pressure-velocity coupled solver. Though the early attempts to develop a coupled solver were unsuccessful due to the huge memory requirements at that time, such algorithms proved to be competitive to the segregated formulation [3,4,5,6,7]. Recently, the authors reported in two separate papers [8,9] a coupled solver that was capable of accelerating the solution of single-phase flow problems by rates reaching about an order of magnitude as opposed to the segregated solver. Their method was nearly grid and under-relaxation independent.

On the other hand, the complexity of the problem is compounded when dealing with multiphase flow problems. The new complexities arise from coupling of the pressure field to several velocity fields and from the inter-fluid drag terms. Also, the increased number of coupled equations adds to the complexity of the problem.

In this paper, the coupled solver, previously developed by the authors, is extended to multiphase flows. The phasic momentum equations and the global pressure equation are grouped in a single matrix that is solved implicitly for all the dependent variables at a time. The pressure velocity coupling is formulated within a collocated, structured grid and using the Mass Conservation Based Algorithm (MCBA) developed by [10].

In the next section, the set of conservation laws governing multiphase flows is introduced, and subsequently discretized. Then the coupled algorithm is briefly explained. Four disperse flow test cases are solved. The performance of the coupled algorithm is compared to SIMPLE in terms of number of iterations and computational time required for convergence.

## 2 GOVERNING EQUATIONS

The equations governing incompressible, steady state, multi-phase flows are the phasic mass conservation equation, the phasic momentum equation, the global continuity equation, and the geometric conservation equation numbered 1 to 4 respectively.

$$\frac{\partial(\rho_k \alpha_k)}{\partial t} + \nabla \cdot (\rho_k \alpha_k \bar{v}_k) = \alpha_k \dot{M}_k \quad (1)$$

$$\frac{\partial(\rho_k \alpha_k \bar{v}_k)}{\partial t} + \nabla \cdot (\rho_k \alpha_k \bar{v}_k \cdot \bar{v}_k) = \nabla \cdot (\mu_k \alpha_k \nabla \bar{v}_k) + \alpha_k (\bar{B}_k - \nabla p) + \sum_{m \neq k} g^{km} (\bar{v}_m - \bar{v}_k) \quad (2)$$

$$\sum_k \frac{\partial(\rho_k \alpha_k)}{\partial t} + \sum_k \nabla \cdot (\rho_k \alpha_k \vec{v}_k) = \sum_k \alpha_k \dot{M}_k = 0 \quad (3)$$

$$\sum_k \alpha_k = 1 \quad (4)$$

In the above equations,  $k$  represents a phase whose density, velocity, and dynamic viscosity are denoted by  $\rho_k$ ,  $\vec{v}_k$  denotes the velocity  $\mu_k$  respectively.  $\alpha_k$  represents the volume fraction of the fluid  $k$  in a certain control volume.  $B_k$  denotes any body force available while  $p$  is the common pressure field.  $g^{km}$  is the interfluid drag coefficient and  $\dot{M}_k$  is the mass source rate.

Generally, the dependent variables in any multi-phase flow problem are the velocity, volume fraction, and pressure fields. The above equations have to be arranged in a way to solve for these variables. In this work, the mass conservation based algorithm (MCBA) is used to solve the resulting system of equations. This algorithm is based upon deriving a pressure correction equation from the global mass conservation equation using the Rhie-Chow approximation technique [11]. Therefore, if the number of available phases is  $N$ ,  $(N-1)$  volume fraction fields are found using  $(N-1)$  phasic mass conservation equations, and the last volume fraction field is found by applying the geometric conservation law. The  $N$  velocity field vectors are found by solving the  $N$  available momentum equations. Table 1 summarizes MCBA for a 2D case.

Equation	Number of Equations	Principal variable	Number of variables
Phasic mass conservation	$N-1$	$\alpha_k$	$N-1$
Momentum conservation	$2N$	$(u_k, v_k)$	$2N$
Global Continuity	$1$	$p$	$1$
Geometric conservation	$1$	$\alpha_N *$	$1$
Total	$3N+1$		$3N+1$

Table 1. MCBA

### 3 FINITE VOLUME METHOD

Each equation in the above set of conservation equations can be cast into a general generic form as

$$\nabla \cdot (\rho \mathbf{v} \phi) = \nabla \cdot (\Gamma \nabla \phi) + Q \quad (5)$$

The meanings of  $\phi$  and  $\Gamma$  differ depending on the equation represented.

In the finite volume method, the domain is discretized by dividing it into a number of control volumes each associated with a main grid point placed at its geometric center. The discretization of the governing conservation equations is accomplished by integrating the general transport equation over the control volume to yield

$$\iint_{\Omega} \nabla \cdot (\rho \mathbf{v} \phi) d\Omega = \iint_{\Omega} \nabla \cdot (\Gamma \nabla \phi) d\Omega + \iint_{\Omega} Q d\Omega \quad (6)$$

Then, using the divergence theorem, the first two volume integrals in equation (6) are transformed into surface integrals that are approximated by the trapezoidal rule over the faces contouring the control volume to yield

$$\sum_{f=nb(P)} (\rho \mathbf{v} \phi - \Gamma \nabla \phi)_f \cdot \mathbf{S}_f = Q_P \Omega_P \quad (7)$$

Using appropriate interpolation schemes, the above semi-discretized equation is transformed to a fully discrete algebraic equation of the form

$$a_P^\phi \phi_P + \sum_{F=NB(P)} a_F^\phi \phi_F = b_P^\phi \quad (8)$$

In this paper, the convection terms are approximated using the first order Upwind scheme, while the diffusion term is interpolated by the second order central difference scheme.

#### 4 COUPLED

Regardless of the solution procedure followed, segregated or coupled, the solution method used in this paper roughly proceeds in two steps:

1. Update the velocity and pressure fields using volume fraction fields from the previous iteration.
2. Use the updated mass flow rate field to find the new volume fraction fields.

In a segregated solver like SIMPLE (which is the algorithm used in this work for comparison), the continuity and momentum equations are decoupled. The momentum equations are used to find the velocity fields assuming known pressure field, and then the continuity equation is solved for the pressure field using the last updated values of velocity. Note that the momentum equations are themselves decoupled from each other in SIMPLE by solving each phasic momentum equation solely for the corresponding phase.

However, in the coupled algorithm, both the velocity and pressure fields are the main variables in the whole set of equations. The momentum equations are solved alongside with the pressure equation simultaneously and for all the available phases.

The solution procedure of a multiphase problem using a coupled algorithm can thus be summarized by the following steps:

1. Start with the most updated values of velocity, pressure and volume fraction field for each phases.

2. Simultaneously solve the system of momentum and pressure equations to update the velocity and pressure fields for all the phases.
3. Update the mass flow rate of each phases at the faces using the Rhie-Chow approximation.
4. Solve the phasic mass conservation equations and update the volume fraction fields.
5. Repeat until convergence.

The detailed discretization for solving single phase flow problems using the coupled algorithm was given in two papers [8, 9]. In this paper, the difference between the single and multiphase problems is pointed out.

Starting with the momentum equation (2), there are two main differences between the multiphase and single phase cases. First, all the terms in the momentum equation are now multiplied by the phasic volume fraction. Second, an interphase drag term appears in the equation. Integrating this term over a control volume such that the velocity of the fluid is considered to prevail inside the control volume

$$\iint_{\Omega} \sum_{m \neq k} g^{km} (\overline{v}_m - \overline{v}_k) d\Omega = \Omega_P \cdot \sum_{m \neq k} g^{km} (\overline{v}_m - \overline{v}_k) \quad (9)$$

This term is added to the coefficients on the left hand side as all the fields are treated implicitly in the coupled formulation.

Since it is derived from the global mass conservation equation, which is the sum of all phasic mass conservation equations, each of the coefficients of the pressure equation represents the sum, over all the available phases, of the coefficient that would show up if each phase was alone. When the discretization is done, at each control volume, a 2-D momentum equation (10) is found. A common pressure equation (11) is also present. Thus if a two-phase flow problem is to be solved, a system of five equations has to be solved for each control volume.

$$\left\{ \begin{array}{l} a_P^{u_k u_k} u_{Pk} + a_P^{u_k v_k} v_{Pk} + a_P^{u_k P} p_P + \sum_{NB} a_{NB}^{u_k u_k} u_{NB,k} + \sum_{NB} a_{NB}^{u_k v_k} v_{NB,k} + \sum_{NB} a_{NB}^{u_k P} p_{NB} + \sum_{m \neq k} a_P^{u_k u_m} u_{Pm} = b_P^{u_k} \\ a_P^{v_k u_k} u_{Pk} + a_P^{v_k v_k} v_{Pk} + a_P^{v_k P} p_P + \sum_{NB} a_{NB}^{v_k u_k} u_{NB,k} + \sum_{NB} a_{NB}^{v_k v_k} v_{NB,k} + \sum_{NB} a_{NB}^{v_k P} p_{NB} + \sum_{m \neq k} a_P^{v_k v_m} v_{Pm} = b_P^{v_k} \end{array} \right. \quad (10)$$

$$\sum_k a_P^{p u_k} u_{Pk} + \sum_k a_P^{p v_k} v_{Pk} + a_P^{pp} p_P + \sum_k \sum_{NB} a_{NB}^{p u_k} u_{NB,k} + \sum_k \sum_{NB} a_{NB}^{p v_k} v_{NB,k} + \sum_{NB} a_{NB}^{pp} p_{NB} = b_P^p \quad (11)$$

When equations (10) and (11) are gathered, for all the control volumes, the solving matrix found is of the form

$$\begin{bmatrix} a_P^{u^k u^k} & a_P^{u^k v^k} & a_P^{u^k u^m} & 0 & a_P^{u^k P} \\ a_P^{v^k u^k} & a_P^{v^k v^k} & 0 & a_P^{v^k v^m} & a_P^{v^k P} \\ a_P^{u^m u^k} & 0 & a_P^{u^m u^m} & a_P^{u^m v^m} & a_P^{u^m P} \\ 0 & a_P^{v^m v^k} & a_P^{v^m u^m} & a_P^{v^m v^m} & a_P^{v^m P} \\ a_P^{Pu^k} & a_P^{Pv^k} & a_P^{Pu^m} & a_P^{Pv^m} & a_P^{PP} \end{bmatrix} \times \begin{bmatrix} u_P^k \\ v_P^k \\ u_P^m \\ v_P^m \\ P_P \end{bmatrix} + \sum_{NB} \begin{bmatrix} a_{NB}^{u^k u^k} & a_{NB}^{u^k v^k} & 0 & 0 & a_{NB}^{u^k P} \\ a_{NB}^{v^k u^k} & a_{NB}^{v^k v^k} & 0 & 0 & a_{NB}^{v^k P} \\ 0 & 0 & a_{NB}^{u^m u^m} & a_{NB}^{u^m v^m} & a_{NB}^{u^m P} \\ 0 & 0 & a_{NB}^{v^m u^m} & a_{NB}^{v^m v^m} & a_{NB}^{v^m P} \\ a_{NB}^{Pu^k} & a_{NB}^{Pv^k} & a_{NB}^{Pu^m} & a_{NB}^{Pv^m} & a_{NB}^{PP} \end{bmatrix} \times \begin{bmatrix} u_{NB}^k \\ v_{NB}^k \\ u_{NB}^m \\ v_{NB}^m \\ P_{NB} \end{bmatrix} = \begin{bmatrix} b_P^{u^k} \\ b_P^{v^k} \\ b_P^{u^m} \\ b_P^{v^m} \\ b_P^P \end{bmatrix} \quad (12)$$

The Coefficients appearing in equations (10), (11), and (12) are summarized in equations (13.1) and (13.2) below

$$\begin{aligned}
a_P^{u^k u^k} &= a_P^{v^k v^k} = \frac{\rho_{kP} \alpha_{kP}^*}{\Delta t} V_P + \sum_f \left\| m_{k,f}, 0 \right\| \alpha_{k,f}^* + \sum_f (\alpha_{k,f}^* \mu_{k,f} \frac{\vec{S} \cdot \vec{S}}{S \cdot d_{PNB}})_f + \sum_{m \neq k} g^{km} V_P \\
a_{NB}^{u^k u^k} &= a_{NB}^{v^k v^k} = - \left\| -m_{kf}, 0 \right\| \alpha_{kNB}^* - (\alpha_{kf}^* \mu_{kf} \frac{\vec{S} \cdot \vec{S}}{S \cdot d_{PNB}})_f \\
a_P^{u^k u^m} &= a_P^{v^k v^m} = g^{km} V_P \\
a_P^{u^k P} &= \sum_f \alpha_{kf}^* r S_{f,x} \\
a_P^{u^k P} &= \sum_f \alpha_{kf}^* (1-r) S_{f,x} \\
a_P^{v^k P} &= \sum_f \alpha_{kf}^* r S_{f,y} \\
a_P^{v^k P} &= \sum_f \alpha_{kf}^* (1-r) S_{f,y} \\
b_P^{u^k} &= \frac{(\rho_P \alpha_{kP}^*)^0}{\Delta t} V_P + \sum_f (\alpha_{kf}^* \mu_{k,f} \nabla u_k \cdot \vec{T})_f + \alpha_{kP}^* B_{k,fx} V_P \\
b_P^{v^k} &= \frac{(\rho_P \alpha_{kP}^*)^0}{\Delta t} V_P + \sum_f (\alpha_{kf}^* \mu_{kf} \nabla v_k \cdot \vec{T})_f + \alpha_{kP}^* B_{k,fy} V_P
\end{aligned} \quad (13.1)$$

$$\begin{aligned}
a_P^{pu_k} &= \sum_f \rho_{kf} \alpha_{kf} r S_{fx} \\
a_{NB}^{pu_k} &= \sum_f \rho_{kf} \alpha_{kf} (1-r) S_{fx} \\
a_P^{pv_k} &= \sum_f \rho_{kf} \alpha_{kf}^* r S_{fy} \\
a_{NB}^{pv_k} &= \sum_f \rho_{kf} \alpha_{kf}^* (1-r) S_{fy} \\
a_P^{pp} &= \sum_k \sum_f \rho_{kf} (\alpha_{kf}^*)^2 \frac{D_f^u E_{fx} + D_f^v E_{fy}}{d_{PF}} \\
a_{NB}^{pp} &= -\sum_k \rho_{kf} (\alpha_{kf}^*)^2 \frac{D_f^u E_{fx} + D_f^v E_{fy}}{d_{PNB}} \\
b_P^p &= \sum_k \sum_f \rho_{kf} (\alpha_{kf}^*)^2 \overline{D_f \nabla p_f^* \cdot \vec{T}_f} - \sum_k \sum_f \rho_{kf} (\alpha_{kf}^*)^2 \overline{D \nabla p_f^* \cdot S_f}
\end{aligned} \tag{13.2}$$

## 5 RESULTS

The aim of this paper is to assess the capability of the coupled algorithm to solve multiphase flow problems. The obtained results are compared to those generated using SIMPLE. The two methods are evaluated based on the solving time and the number of iterations needed to reach convergence.

The test cases solved are all of the same geometry shown in figure 1. The physical domain is 20m long. In all the cases, the inlet conditions of phasic velocities and volume fractions are known. The gauge pressure at the outlet is always set to 0.

The test cases are solved over quadrilateral meshes of densities 10000, 30000, and 50000 elements respectively.

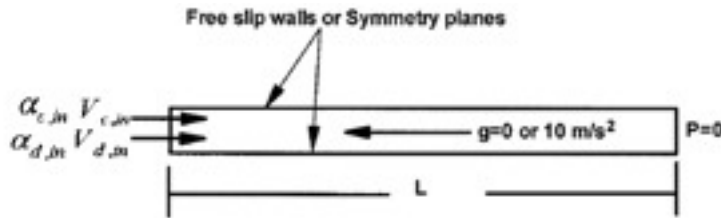


Figure 1. The physical domain

The different test cases are broadly grouped into two main categories: horizontal and vertical bubbly flows. The vertical cases are solved in the same physical domain (figure 1) by setting the gravity field to  $\vec{g}(-10;0)$ .

In all the cases, the steady flow of air bubbles in a stream of water is studied. The drag force between the two phases now appears in the equations, and the interfluid drag coefficient is given by:

$$g^{km} = \frac{3}{4} \frac{CD}{d_p} \alpha_d \rho_c V_{slip} \quad (14)$$

In equation 13, The subscripts  $c$  and  $d$  in the above relation denote the continuous (i.e. water) and disperse (i.e. air) phases respectively. The parameter  $d_p$  is the particle diameter.  $V_{slip}$  is the slip velocity, which results from the difference in velocities between the two phases, and is given by:

$$V_{slip} = \sqrt{(u_d - u_c)^2 + (v_d - v_c)^2} \quad (15)$$

$$\text{CD is defined as } CD = \frac{24}{R_{ep}} + 0.44 \quad \text{where } R_{ep} = \frac{d_p V_{slip}}{\nu_c} \quad (16)$$

At the state of convergence and for the horizontal test cases, the two phases are expected to reach an equilibrium velocity

$$V_{equilibrium} = \alpha_{d,in} V_{d,in} + \alpha_{c,in} V_{c,in} \quad (17)$$

The variables in the above relation denote the volume fraction and the velocity of each phase at inlet and are specified for each case.

A test case is considered converged when the maximum residual reached is  $10^{-5}$  for both the coupled and segregated approaches. The maximum residual for each equation is computed as

$$RES = \max_{i=1}^{NE} \frac{\left| a_p \phi_p + \sum_{NB} a_{NB} \phi_{NB} - b_p \right|}{a_p \phi_p} \quad (18)$$

It is worth noting that in each of the cases, a false transient term is used to promote the convergence of the coupled algorithm. A similar term, as well as an under-relaxation term, are used together in the case of SIMPLE.

## 5.1 Horizontal Bubbly flow:

### 5.1.1 Dilute Bubbly Flow:

In this case  $V_{c,in} = 5 \text{ m/s}$ ,  $V_{d,in} = 1 \text{ m/s}$ ,  $\alpha_{d,in} = 0.1$  and  $\alpha_{c,in} = 0.9$ . The other properties are  $d_p = 2 \text{ mm}$ ,  $\rho_c = 1000 \text{ kg.m}^{-3}$  and  $\rho_d = 1 \text{ kg.m}^{-3}$ . The viscosity of water is  $\mu_c = 10^{-3} \text{ Pa.s}$ .

The equilibrium velocity as depicted by equation (17) is 4.6 m/s. Due to the large difference in densities, both phases reach the equilibrium velocity over a very short distance from the inlet.

Figure 2 shows the two phases velocities as function of  $x$  for the coupled and segregated algorithms.



As for the comparison of the number of iterations required by each algorithm to reach convergence, the coupled algorithm requires much less iterations over each grid density than the segregated. A more detailed comparison of the performance of the two algorithms is shown in table 2.

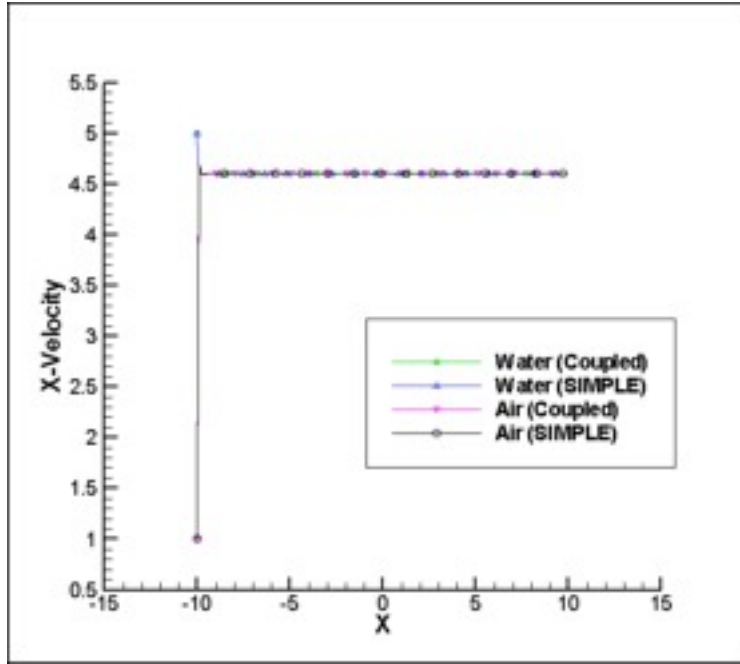


Fig 2. Dilute horizontal bubbly flow – Velocity Profiles

Mesh (x 10 <sup>3</sup> )	Coupled Solver		Segregated Solver		Reduction (%)	
	Number of iterations	Solving time (s)	Number of iterations	Solving time (s)	Number of Iterations	Solving Time
10	35	262.22	450	592.95	-92.2	-55.78
30	34	843.27	637	2580.7	-94.7	-67.3
50	39	1360.6	640	4593.3	-93.9	-70.4

Table 2 Dilute horizontal bubbly flow – convergence comparison

As shown in the above table, the coupled algorithm saves up to 70% of the solution time in the case of 50000 elements grid. The coupled solver is much less dependent on the grid density than SIMPLE.

### 5.1.2 Dense Bubbly flow:

The parameters in this case are just as those in the previous one except that  $\alpha_{d,in} = 0.4$ .

At such a high void volume fraction, bubble coalescence may occur, but this is not accounted for in this paper. The equilibrium velocity as determined by equation (16) is 3.4 m/s. As seen in figure (3) both algorithms give an exact estimate of this velocity.

Table 3 shows a comparison between the performances of coupled and SIMPLE algorithms. For the 50000 elements grid, the coupled solver faces relative difficulty in the convergence.

This case is to be examined in further work. Note that, however, for the 30000 elements case, the coupled saves about 77% of the solving time as compared to SIMPLE.

Mesh (x 10 <sup>3</sup> )	Coupled Solver		Segregated Solver		Reduction (%)	
	Number of iterations	Solving time (s)	Number of iterations	Solving time (s)	Number of Iterations	Solving Time
10	49	282.4	510	670.81	-90.4	-57.9
30	51	899.23	959	3891.47	-94.7	-76.9
50	93	3410.9	1445	9798.83	-93.6	-65.2

Table 3. Dense horizontal bubbly flow – convergence comparison

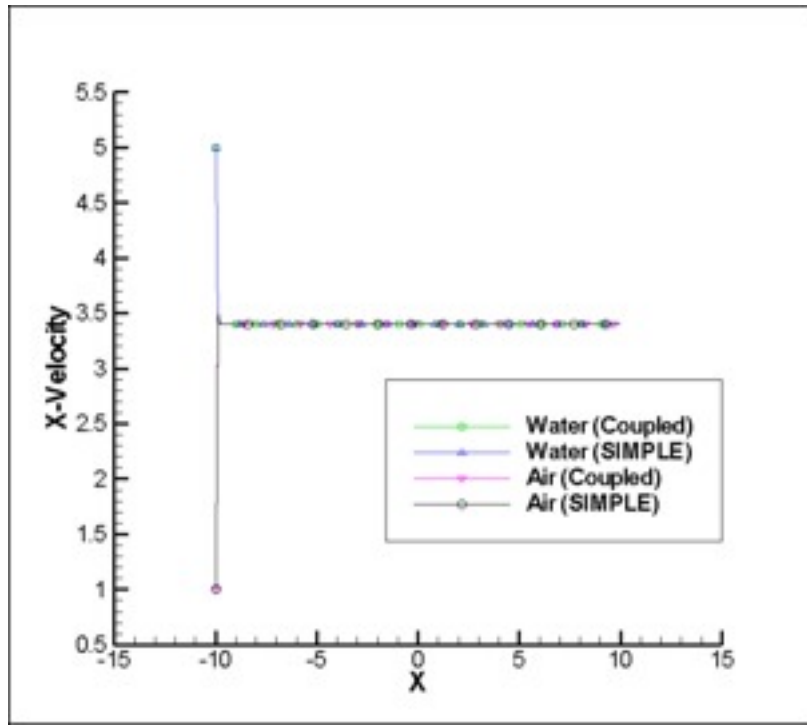


Fig. 3 Dense horizontal bubbly flow – velocity profiles

## 5.2 Vertical Bubbly Flows

In this case, the direction of flow is vertical. The same physical field shown in figure 1 is used with the gravitational force equal to  $-10 \text{ m/s}^2$  in the x-direction. The equilibrium velocity cannot be accurately estimated by equation (17) due to the presence of the gravitational field. However, these cases are in great accordance with the results published in [12].

### 5.2.1 Dilute Bubbly Flow:

The flow parameters for this problem are set as follows

$$V_{c,in} = 100m/s, V_{d,in} = 10m/s, \alpha_{d,in} = 0.1 \text{ and } \alpha_{c,in} = 0.9$$

$$d_p = 2mm, \rho_c = 1000 kg.m^{-3} \text{ and } \rho_d = 1 kg.m^{-3}$$

Figure 4 shows the profiles of velocity for both phases. The curves of both the coupled and segregated formulations lie on top of each other. Table 4 compares the performances of both algorithms. In this case, the coupled solver, once more, proves to be less grid dependent than the segregated solver. The solution of the problem is achieved by the coupled solver in fifth of the time required by SIMPLE for the 50000 case.

Mesh (x 10 <sup>3</sup> )	Coupled Solver		Segregated Solver		Reduction (%)	
	Number of iterations	Solving time (s)	Number of iterations	Solving time (s)	Number of Iterations	Solving Time
10	33	196.21	476	603.8	-93.1	-67.5
30	53	1086.7	914	3757.65	-94.2	-71.1
50	59	2069.5	1400	9454.2	-95.8	-78.1

Table 4 Dilute vertical bubbly flow – convergence comparison

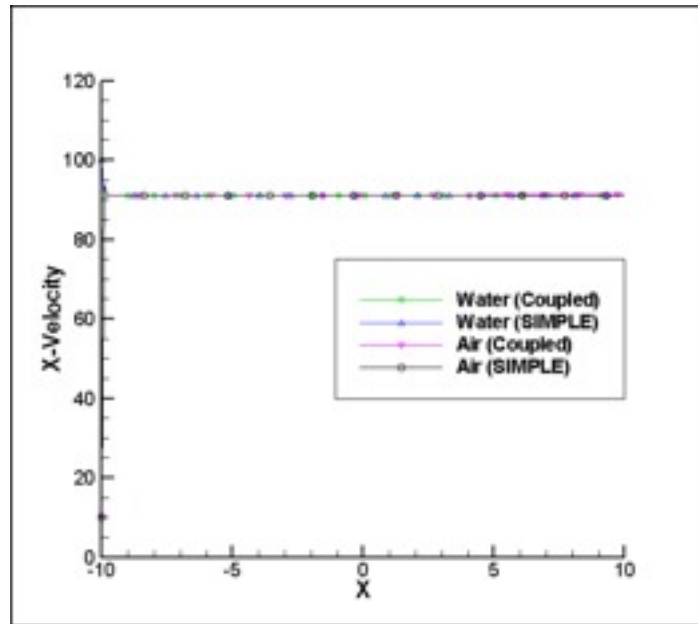


Figure 4 Dense vertical bubbly flow – velocity profiles

### 5.2.2 Dense Bubbly Flow:

The conditions are kept similar to those in the previous test case, but the inlet volume fraction of the disperse phase is set to  $\alpha_{d,in} = 0.4$ . Most of the inertia is carried by the solid phase. Figure 5 shows the axial velocity as a function of x. Both algorithms give the same numerical solution. Table 5 shows a comparison between the two algorithms. Note that for this particular case, the coupled algorithm is not at all grid independent. Investigation of

this behavior in this case is to be conducted. Nevertheless, the coupled solver still saves tremendous time as compared to SIMPLE in all the cases.

Mesh (x 10 <sup>3</sup> )	Coupled Solver		Segregated Solver		Reduction (%)	
	Number of iterations	Solving time (s)	Number of iterations	Solving time (s)	Number of Iterations	Solving Time
10	35	265.9	477	626.75	-92.7	-57.6
30	128	2149.9	904	3838.1	-85.8	-44
50	175	6418.4	1389	9277.1	-87.4	-30.8

Table 5 Dense vertical bubbly flow – convergence comparison

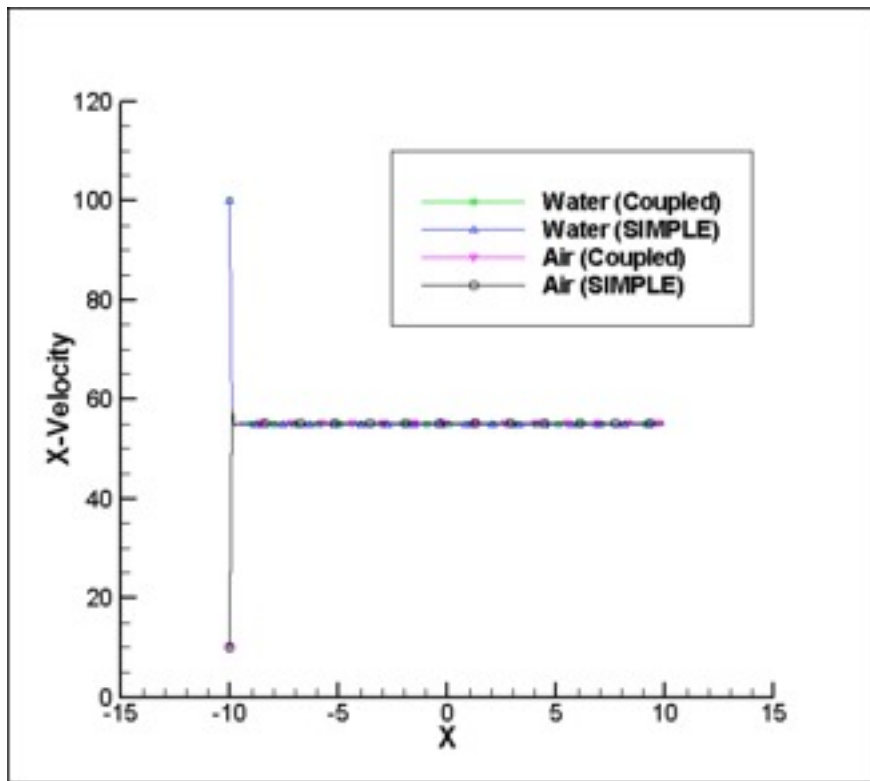


Figure 5 Dense vertical bubbly flow – velocity profiles

## 6 CONCLUSIONS

This paper shows the efficiency of the coupled solver in solving multiphase disperse flow problems as compared to the segregated SIMPLE algorithm. However, the test cases used in this paper are all 1-dimensional. The following points are left for future work:

- The strange behavior of the coupled algorithm in the case of dense cases is to be investigated thoroughly.
- 2-dimensional problems are to be tested in order to assess the ability of the coupled solver to solve such problems.
- The phases in the presented problems are all incompressible. In future, a coupled solver capable to simulate compressible multiphase flows is to be developed.
- In our work, the volume fraction field is not coupled with the pressure and velocity. A fully coupled multiphase flow solver is to be developed.
- In some cases, we faced problems with the multigrid solver used. This is an issue that warrants further investigation.

## 7 REFERENCES

1. Patankar, S. V. and Spalding, D. B., "A Calculation Procedure for Heat, Mass and Momentum Transfer in Three-Dimensional Parabolic Flows," *Int. Journal of Heat and Mass Transfer*, **15**, 1787-1806 (1972).
2. Moukalled, F. and Darwish, M., "A Unified Formulation of the Segregated Class of Algorithms for Fluid Flow at All Speeds," *Numerical Heat Transfer, Part B*, **37**, 103-139 (2000).
3. Caretto, L. S., Curr, R. M., and Spalding, D. B., "Two Numerical Methods for Three - Dimensional Boundary Layers," *Computer Methods in Applied Mechanics and Engineering*, **1**, 39-57 (1972).
4. Vanka, S. P., Block-Implicit Multigrid Solution of Navier-Stokes Equations in Primitive Variables," *Journal of Computational Physics*, **65**, 138-158 (1986).
5. Karki, K. C. and Mongia, H. C., "Evaluation of a Coupled Solution Approach for Fluid Flow Calculations in Body Fitted Co-ordinates," *International Journal for Numerical Methods in Fluids*, **11**, 1-20 (1990).
6. Braaten, M. E., Development and Evaluation of Iterative and Direct Methods for the Solution of the Equations Governing Recirculating Flows, PhD. Thesis, University of Minnesota, May 1985.
7. Mazhar, Z., "A Procedure for the Treatment of the Velocity-Pressure Coupling Problem in Incompressible Fluid Flow," *Numerical Heat Transfer, Part B*, **39**, 91-100 (2001).
8. M. Darwish, I. Sraj, and F. Moukalled, A Coupled Incompressible Flow Solver on Structured Grids, *Numerical Heat Transfer, Part B*, **52**, 353-371 (2007).

9. M. Darwish, I. Sraj, and F. Moukalled, "A Coupled Finite Volume Solver for the Solution of Incompressible Flows on Unstructured Grids", *J. of Comput. Physics*, **228**, Issue 1, pp. 180-201 (2009).
10. Darwish, M., Moukalled, F., and Sekar, B., "A Unified Formulation of the Segregated Class of Algorithms for Multi-Fluid Flow at All Speeds," *Numerical Heat Transfer; part B*, **40**, 99-137 (2001).
11. C. M. Rhie and W. L. Chow, "A Numerical Study of the Turbulent Flow Past an Isolated Airfoil with Trailing Edge Separation," *AIAA J.*, **21**, 1525-1532 (1983).
12. Moukalled, F. and Darwish, M., "A Comparative Assessment of the Performance of Mass Conservation Based Algorithms for Incompressible Multi-Phase flows," *Numerical Heat Transfer; Part B*, **45**, 49-74 (2004).